
Inter-Level Cooperation in Hierarchical Reinforcement Learning

Abdul Rahman Kreidieh, Glen Berseth, Brandon Trabucco, Samyak Parajuli,
Sergey Levine, Alexandre M. Bayen
University of California, Berkeley

Abstract

Hierarchical models for deep reinforcement learning (RL) have emerged as powerful methods for generating meaningful control strategies in difficult long time horizon tasks. Training of said hierarchical models, however, continue to suffer from instabilities that limit their applicability. In this paper, we address instabilities that arise from the concurrent optimization of goal-assignment and goal-achievement policies. Drawing connections between this concurrent optimization scheme and communication and cooperation in multi-agent RL, we redefine the standard optimization procedure to explicitly promote cooperation between these disparate tasks¹. Our method is demonstrated to achieve superior results to existing techniques in a set of difficult long time horizon tasks, and serves to expand the scope of solvable tasks by hierarchical reinforcement learning. Videos of the results are available at: <https://sites.google.com/berkeley.edu/cooperative-hrl>.

1 Introduction

In order for agents to solve interesting problems in the real world they need to be capable of discovering solutions to long and complex planning problems. Due to the challenges of estimating expectations over long sequences and performing efficient exploration, however, RL has had limited success in solving long horizon planning problems [1, 2, 3] without additional temporal structure.

In response to the above limitation, hierarchical models for neural networks, such as feudal networks [4] and its variants [5, 3, 6] propose methods for decomposing complex tasks into simpler sub-problems that are more manageable to solve using low-level action primitives. These models do so by breaking apart the policy into a sequence of temporally abstracted sub-policies, thereby allowing for higher level policies to more easily perceive the effects of actions over larger time intervals. The actions of the higher level policies are passed to the levels below them as a goal, and the low-level policies are then trained to achieve these goals via a goal-conditioned reward function over smaller time horizons.

While hierarchical policies improve exploration and reduce the effective learning horizon of a given task via temporal abstraction, such models decompose the policy into a set of independent actors that solve disparate optimization problems. This renders hierarchical policy optimization similar to *multi-agent reinforcement learning* (MARL) [7, 8], which results in training challenges of its own [9, 10, 11], notably non-stationarity [12, 13, 14] and mixed cooperative and competitive behaviors [15, 16, 17]. While previous studies have accounted for non-stationarity in HRL [3, 6], this paper focuses on a separate connection between hierarchical and multi-agent RL, namely the concept of utilizing communication for facilitating intra-agent cooperation [18, 10]. In MARL, communication channels are often shared among agents as a means of coordinating and influencing

¹For the purposes of reproducibility, the presented algorithms, environments, and results are available online at: <https://github.com/AboudyKreidieh/h-baselines>.

neighboring agents. Challenges emerge, however, as a result of the ambiguity of communication signals in the early staging of training, with agents forced to coordinate between sending and interpreting messages [19, 20]. Similar communication channels are present in the HRL domain, with higher-level policies communicating one-sided signals in the form of goals to lower-level policies. The difficulties associated with cooperation, accordingly, likely persist under this setting. In particular, at the early stages of training, lower-level policies are unable to perform any goal assigned to them by a higher-level policy, and instead must learn to do so as training progresses. This serves to exacerbate the difficulty of the optimization procedure from the perspective of the higher-level policy, which is unable to identify whether a specific goal under-performed as a result of the choice of goal or the lower-level policy’s inability to achieve it.

Motivated by studies on differentiable communication [21, 22] and emergent cooperation phenomena [16, 23] in MARL, the present article proposes a novel optimization procedure to address limitations associated with inter-level cooperation in HRL. Our approach attempts to encourage cooperation between various levels of a hierarchy by redefining the objective of higher-level policies to directly account for losses experienced by lower-level policies, thereby allowing the policy to disambiguate goals with small expected returns from goals that were unachievable by the lower-level policy. The gradients associated with these additions to the loss of the higher-level policies are then propagated through its parameters by replacing the communication actions (or goals) by the higher-level policy during training with direct connections between its output and the input to the lower-level policy.

The key contributions of this paper are as follows:

- We derive a new off-policy gradient algorithm for higher level policies in two-level hierarchical policies. Our technique, called *Cooperative HiErarchical RL* (CHER), is empirically demonstrated to achieve superior performance on a variety of long-term horizon tasks, and further serves to expand the scope of solvable tasks by hierarchical reinforcement learning.
- Key to our technique is the ability to control the amount of cooperation between the HRL layers. As a result, we dedicate a portion of this paper on developing an intuition of the effects this particular cooperation mechanism can have on the evolution of the various levels.

The remainder of the paper is organized as follows. Section 2 provides background on MDPs, reinforcement learning, and HRL, and presents the hierarchical model utilized for the rest of the paper. Section 3 introduces the CHER algorithm and compares it to the standard goal-conditioned optimization scheme. Section 4 finds connections with our work and others involving improved coordination with gradients, and draws similarities between insights from state-of-the-art HRL algorithms and methods for improving training performance in MARL domains. And finally, Section 5 empirically compares our model with other hierarchical algorithms for various long horizon control and planning tasks ranging from agent navigation to mixed-autonomy traffic flow control.

2 Background

2.1 Reinforcement learning and MDPs

RL problems are generally studied as a *Markov decision problem* (MDP) [24], defined by the tuple:

$$\text{MDP} = (\mathcal{S}, \mathcal{A}, \mathcal{P}, r, \rho_0, \gamma, T) \tag{1}$$

where $\mathcal{S} \subseteq \mathbb{R}^n$ is an n -dimensional state space, $\mathcal{A} \subseteq \mathbb{R}^m$ an m -dimensional action space, $\mathcal{P} : \mathcal{S} \times \mathcal{A} \times \mathcal{S} \rightarrow \mathbb{R}_+$ a transition probability function, $r : \mathcal{S} \rightarrow \mathbb{R}$ a bounded reward function, $\rho_0 : \mathcal{S} \rightarrow \mathbb{R}_+$ an initial state distribution, $\gamma \in (0, 1]$ a discount factor, and T a time horizon.

In a MDP, an *agent* is in a state $s_t \in \mathcal{S}$ in the environment and interacts with this environment by performing actions $a_t \in \mathcal{A}$. The agent’s actions are often defined by a policy $\pi_\theta : \mathcal{S} \times \mathcal{A} \rightarrow \mathbb{R}_+$ parametrized by θ . The objective of the agent is to learn an optimal policy: $\theta^* := \operatorname{argmax}_\theta \eta(\pi_\theta)$, where $\eta(\pi_\theta) = \sum_{i=0}^T \gamma^i r_i$ is the expected discounted return.

2.2 Hierarchical reinforcement learning

In HRL, the policy is decomposed into a high-level policy that optimizes the original task reward, and a low-level policy that is conditioned on latent goals from the high-level and executes actions

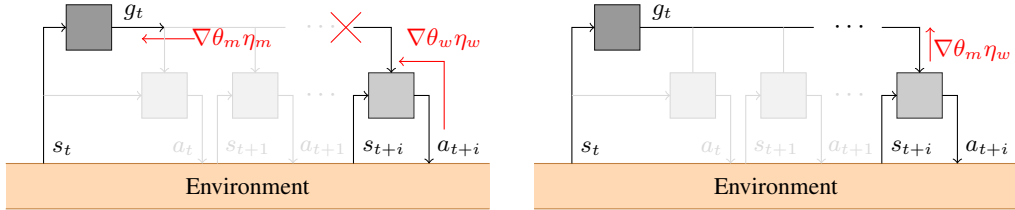


Figure 1: A schematic representation of the hierarchical model and policy gradients. The high-level manager issues goals g_t every k time steps to the low-level worker. The worker then perform actions a_t to accomplish these goals. **Left:** The actors for each level are trained to maximize separate rewards, as indicated by the gradients in red. No gradients are shared between them. **Right:** To encourage cooperation between the policies, we propose the inclusion of a gradient term that propagates the rewards associated with the worker policies through the manager as well.

within the environment. The high-level controller is decoupled from the true MDP via by operating at a lower temporal resolution and passing goals [4] or options [25] to the lower-level. This can reduce the credit assignment problem from the perspective of the high-level controller, and allows the low-level policy to produce action primitives that support short time horizon tasks as well.

Several HRL frameworks have been proposed to facilitate and/or encourage the decomposition of decision-making and execution during training [25, 4, 26, 27]. In this paper, we consider a two-level goal-conditioned arrangement (see Figure 1 (top left)). This network consists of a high-level, or manager, policy π_m that computes and outputs goals $g_t \sim \pi_m(s_t)$ every k time steps, and a low-level, or worker, policy π_w that takes as inputs the current state and the assigned goals and is encouraged to perform actions $a_t \sim \pi_w(s_t, g_t)$ that satisfy these goals via an intrinsic reward function $r_w(s_t, g_t, s_{t+1})$ (see Appendix E.3).

3 Cooperative hierarchical reinforcement learning

In this section, we introduce CHER. We begin by defining the HRL optimization scheme used in prior work, and describe limitations associated with this naive procedure. We subsequently attempt to resolve these limitations in Section 3.2.

3.1 Naive HRL optimization

We begin by providing an explicit definition of the (naive) concurrent training procedure between the manager and worker policies. Under standard formulations of the goal-conditioned HRL optimization scheme, the manager in this setting is rewarded based on the original environmental reward function: $r_m(s_t)$. The objective function from the perspective of the manager is then:

$$\eta_m = \mathbb{E}_{s \sim p_\pi} \left[\sum_{t=0}^{T/k} [\gamma^t (r_m(s_t, \pi_m(s_t)))] \right] \quad (2)$$

Unlike the manager, the worker policy is motivated to follow the goals set by the manager via an intrinsic reward $r_w(s_t, g_t, s_{t+1})$ separate from the external reward. The objective function from the perspective of the worker is then:

$$\eta_w = \lambda \mathbb{E}_{s \sim p_\pi} \left[\sum_{t=0}^k \gamma^t r_w(s_t, g_t, \pi_w(s_t, g_t)) \right] \quad (3)$$

The update procedures for each policy are depicted in Fig. 1 (bottom left). Notably, no gradients under this formulation are shared between the manager and worker policies. The absence of loss sharing results in a situation whereby the manager policy does not receive direct feedback on an agent’s ability to perform certain goals, a factor that can have a significant impact on the value of the specified goal. This serves to exacerbate the hierarchical credit assignment problem [28]. The unconstrained nature of the manager’s evolution can also result in situations whereby the worker policy chases an unstable target as the manager attempts to identify effective goals. Such phenomena are widely known sources of training instabilities in various domains of deep reinforcement learning [29].

3.2 Promoting cooperation via loss-sharing

In order to alleviate the training challenges described in the previous subsection, this paper redefines the higher-level objective function to directly promote cooperation by the manager policies with the policy directly below it. Cooperation within this setting is promoted by incorporating a weighted form of the worker expected return to the original manager policy η_m . Our new expected return is:

$$\eta'_m = \eta_m + \lambda\eta_w = \mathbb{E}_{s \sim p_\pi} \left[\sum_{t=0}^{T/k} [\gamma^t (r_m(s_t, \pi_m(s_t)))] \right] + \lambda \mathbb{E}_{s \sim p_\pi} \left[\sum_{t=0}^k \gamma^t r_w(s_t, g_t, \pi_w(s_t, g_t)) \right] \quad (4)$$

where λ is a weighting term that controls the level of cooperation the manager has with the worker. This term is in part motivated studies on the dynamics and evolution of cooperative behaviors in MARL, and is to a certain extent similar to cooperative reward scheme ρ in [15]. As we present in Section 5.4, this term can have a significant effect of training performance.

To compute the gradient of the additional weighted expected return through the parameters of the manager policy, we take inspiration from similar studies in differentiable communication in MARL. The main insight that enables the derivation of such a gradient is the notion that goal states g_t from the perspective of the worker policy are structurally similar to communication signals in multi-agent systems. As a result, the gradients of the expected intrinsic returns can be computed by replacing the goal term within the reward function of the worker with the direct output from the manager’s policy, a technique that was initially adopted in [22]. The updated gradient is defined in Theorem 1 below.

Theorem 1. *Define the goal g_t provided to the input of the worker policy $\pi_w(s_t, g_t)$ as the direct output from the manager policy g_t whose transition function is:*

$$g_t(\theta_m) = \begin{cases} \pi_m(s_t) & \text{if } t \bmod k = 0 \\ h(s_{t-1}, g_{t-1}(\theta_m), s_t) & \text{otherwise} \end{cases} \quad (5)$$

where $h(\cdot)$ is a fixed goal transition function between meta-periods (see Appendix E.3). Under this assumption, the solution to the deterministic policy gradient [30] of Eq. (4) with respect to the manager policy’s parameters θ_m is:

$$\begin{aligned} \nabla_{\theta_m} \eta'_m(\theta_m) = & \mathbb{E}_{s \sim p_\pi} \left[\nabla_a Q_m(s, a) \Big|_{a=\pi_m(s)} \nabla_{\theta_m} \pi_m(s) \right] \\ & + \lambda \mathbb{E}_{s \sim p_\pi} \left[\nabla_{\theta_m} g_t \nabla_g (r_w(s_t, g, \pi_w(s_t, g_t)) + \pi_w(s_t, g) \nabla_a Q_w(s_t, g_t, a) \Big|_{a=\pi_w(s_t, g_t)}) \Big|_{g=g_t} \right] \end{aligned} \quad (6)$$

where $Q_m(s, a)$ and $Q_w(s, g, a)$ are approximations for the expected environmental and intrinsic returns, respectively.

Proof. See Appendix A.

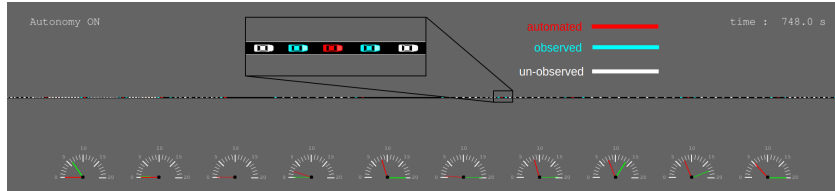
We limit our derivation of the cooperative gradient to deterministic policy gradients as it a commonly studied RL algorithm in recent studies on HRL [6, 3, 31], and as a result allows us to fairly compare the use of cooperation-inducing losses to existing state-of-the-art methods. The derivation of this gradient to direct policy gradient [32] and soft actor-critic [33] methods is a topic of future work.

Breaking this new gradient apart, we can see that it consists of three terms. The first and third term computes the gradient of the critic policies Q_m and Q_w with respect to the parameters θ_m , respectively. The second term computes the gradient of the worker-specific reward with respect to the parameters θ_m . While this second term at first glance may seem unusual, it is worth remembering that this reward function is in fact a design feature within the HRL formulation to assist in learning helpful lower-level control. We describe a practical algorithm for training a cooperative two level hierarchy implementing this loss function in Algorithm 1.

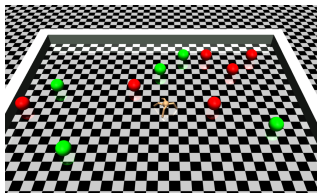
4 Related Work

One prominent limiting factor in multi-agent training is the notion of *non-stationarity* [12, 13, 14], whereby the continually changing nature of decision-making policies with respect to one another serve to destabilize training². This has been identified and addressed in previous studies on HRL, with techniques such as off-policy sample relabeling [3] and hindsight [6] providing considerable

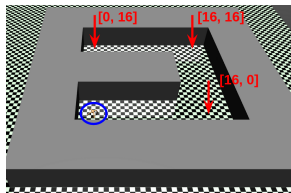
²The notion of non-stationarity in HRL and its connection to MARL is expanded upon in Appendix B.



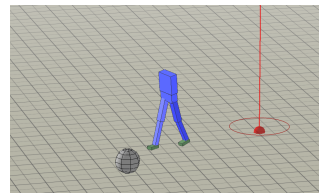
(a) Single-Lane Highway



(b) Ant Gather



(c) Ant Maze



(d) Bipedal Soccer

Figure 2: Training environments explored within this paper. We compare the performance of various HRL algorithms on a mixed-autonomy traffic control task (a), two ant navigation tasks (b,c), and a bipedal/humanoid navigation task (d). A description of each of these environments is provided in Section 5.1.

improvements to training performance. Similarly, the method presented in this paper can be seen as a means of addressing non-stationarity in HRL, with the manager constraining its search within the region of achievable goals by the worker. Unlike these methods, however, our approach additionally accounts for ambiguities with respect to the credit assignment problem from the perspective of the higher level policy, and as such are likely to be more beneficial when utilizing on-policy RL algorithms, in which non-stationarity is usually resolved via optimization schemes that constraint the KL divergence between subsequent updates [34, 35, 36]. Finally, our approach is not exclusive from existing state-of-the-art methods, but rather can improve the performance of any HRL method that relies on standard policy update procedures. This discussed in Appendix F.1.

Our work is related to communication in multi-agent systems in works such as [37, 38, 21] and namely is most similar to the Differentiable Inter-Agent Learning (DIAL) method proposed in [22]. Our work does not aim to learn an explicit communication channel; however, it is motivated by a similar principle - that letting gradients flow across agents results in richer feedback. Furthermore, we differ in the fact that we structure the problem as a hierarchical reinforcement learning with temporal abstraction, forcing a more constrained and directed objective. Finally, our gradients are propagated from the worker up to the manager and not arbitrarily among agents.

5 Experiments

In this section, we detail the experimental setup and training procedure, and present results of various continuous control tasks. In these experiments we want to determine two things, (1) does information sharing via the communication channel between the HRL layers improve performance and (2) can using this cooperation method increase the scalability of HRL to new complex control tasks.

5.1 Environments

The performance of the proposed method is demonstrated on a suite of long horizon control and planning tasks. We briefly describe these tasks below; additional environment details can be found in Appendix D.

Ant Gather In this task shown in Figure 2b, an agent is placed in a 20×20 space with 8 apples and 8 bombs. The agent receives a reward of +1 or collecting an apple (denoted as a green disk) and -1 for collecting a bomb (denoted as a red disk); all other actions yield a reward of 0.

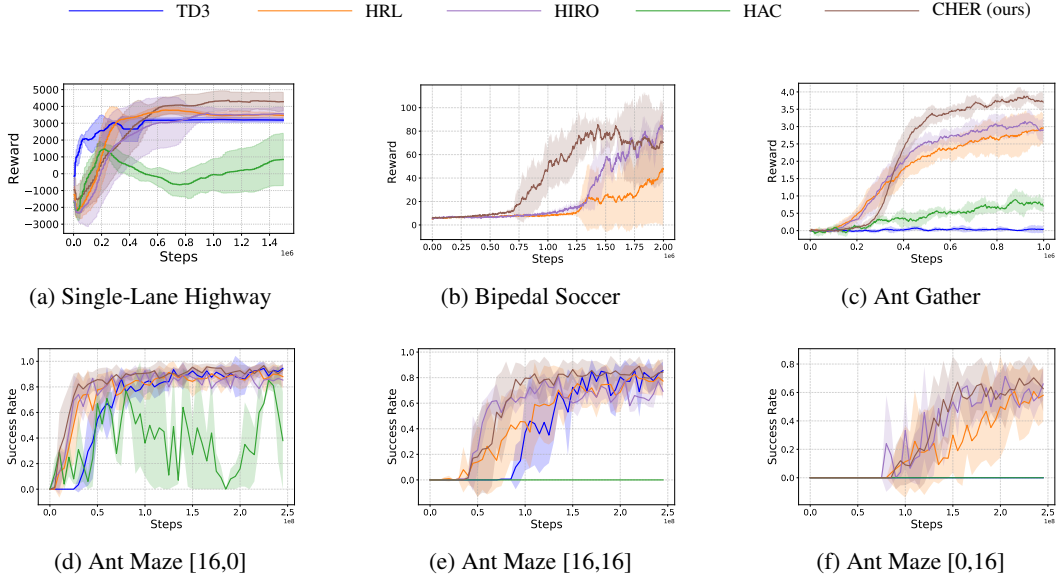


Figure 3: Training performance of the different algorithms on various environments.

Ant Maze For this task, immovable blocks are placed to confine the agent to a U-shaped corridor, shown in Figure 2c. The agent is initialized at position $(0, 0)$, and assigned an (x, y) goal position in the corridor. The agent receives reward defined as the negative L_2 distance from this (x, y) position.

Bipedal Soccer A bipedal agent is placed in an open field with a soccer ball. The agent is rewarded for moving to the ball, and additionally dribbling the ball to the target. The reward function is the distance of the ball from a desired goal position shown in Figure 2d. This reward is positive to discourage the agent from falling prematurely [39].

Single-Lane Highway In addition to various agent navigation tasks, we explore the use of goal-conditioned hierarchies on a mixed-autonomy traffic control, see Figure 2a. This task consists of a single lane highway in which downstream traffic instabilities generate congestion in the form of stop-and-go waves, represented by the red diagonal lines in Figure 4b. During training, a subset of vehicles within a controllable region are replaced with automated vehicle whose actions (in this case desired accelerations) are sampled from a centralized policy. The vehicles are incentivized to reduce congestion within the network via a objective function that rewards high global speeds and penalizes large accelerations by the automated vehicles.

5.2 Experimental setup

Experiments were conducted using the TD3 as the underlying learning algorithm [40], a variant of the DDPG [41] algorithm for continuous control that utilizes dual value functions and delaying policy updates to reduce overestimation bias. All results are reported over 10 random seeds. For more details on the hyper-parameters used see Appendix E.1.

5.3 Comparative analysis

We test our proposed algorithm against the following baseline methods:

- **TD3**: In order to validate the need for goal-conditioned hierarchies to solve our tasks, we compare all results against a fully connected network with otherwise similar network/training configurations.
- **HRL**: This baseline consists of the naive formulation of the hierarchical reinforcement learning optimization scheme (see Section 3.1). This is analogous to the CHER algorithm with λ set to 0.
- **HIRO**: Presented in [3], this method addresses the non-stationarity effects between the manager and worker policies by relabeling the manager actions (or goals) to render actual observed action sequence more likely to have happened with respect to the current instantiation of the worker policy.

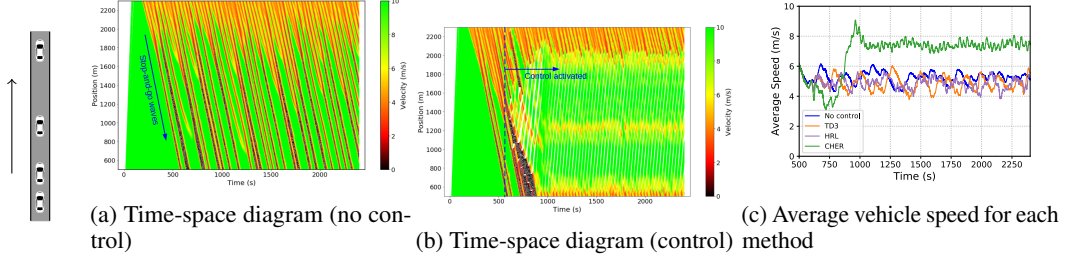


Figure 4: Traffic flow performance of vehicles within the Single-Lane Highway environment. The time-space diagrams depict the trajectories of individual vehicles through the network, and are colored by the instantaneous speeds of vehicles to further elucidate the effects specific driving behaviors. **a)** In the absence of control, downstream traffic instabilities result in the propagation of congestion in the form of stop-and-go waves, seen as the red diagonal streaks. **b)** The control strategy generated via CHER results in vehicles forming gaps that prevent these waves from propagating fully through the network. **c)** This behavior provides significant improvements to average speed of vehicle within the controllable edge; in contrast, other methods are unable to improve upon the uncontrolled (fully human-driven) baseline.

This is done by sampling a sequence of potential goals via a Gaussian centered at $s_{t+k} - s_t$ and choosing the candidate goal that maximizes the log-probability of the actions that were originally performed by the worker. The reproducibility of this algorithm is addressed in Appendix E.4.

- *HAC*: Similar to the HIRO algorithm, the HAC algorithm [6] attempts to address non-stationarity in off-policy learning by replaying sampled data. In this case, they train their high level policy with special hindsight action and goal transitions from an optimal lower-level policy as well as using subgoal testing transitions to prevent learning from a restricted set of subgoal states. Implementation details and modifications to this algorithm are provided in Appendix E.5.

For our algorithm, CHER, we set $\lambda = 0.01$ for the Ant Gather and Bipedal Soccer environments, $\lambda = 0.005$ for the Ant Maze environment, and $\lambda = 0.02$ for the Single-Lane Highway environment.

We first perform a sample efficiency study designed to examine how effective CHER is compared to related methods. Figure 3 depicts the training performance of each algorithm for the various environments described in the Section 5.1. In many cases, the use of cooperative higher-level objectives empirically provides significant improvements on the optimal performance of the policy within the environment. In the Ant Gather and Single-Lane Highway environments, while the CHER policy originally progresses more slowly than standard HRL, it is ultimately capable of outperforming all other policies, producing a maximum return of 4.10 ± 0.18 and 4546 ± 431 , respectively, across 10 policies. This serves to far exceed the standard HRL algorithm’s maximum return of 3.04 ± 0.54 and 3852 ± 200 , respectively. The CHER algorithm also exhibits more stable training in this Ant Gather environment, yielding a much smaller variance in performance between seeds.

In the Single-Lane Highway environment in particular, CHER enables the generation of meaningful traffic flow control behaviors by the automated vehicles, as seen in Figure 4b. This is in stark contrast to the non-hierarchical and standard HRL approaches, in which the learned control strategies do not result in significant improvements to the traveling speed of traffic, as seen in Figure 4c. These results indicate that CHER has (1) improved over current methods, and (2) expanded the space of control tasks that can be solved with HRL methods.

Similar improvements can be seen in the Ant Maze tasks in Figure 3(d-f). In this case, CHER performs approximately equivalently to the HRL algorithm for simple goals, in this case moving to (16,0), i.e. simply moving forward. However, for the more difficult tasks CHER converges several hundreds of thousands of steps prior to the standard HRL approach, and is comparable to the HIRO algorithm in terms of sample efficiency. Unlike HIRO, CHER does not rely on relabeling techniques that are computationally expensive, and CHER achieves greater evaluation performance than HIRO, at a lower wall-clock time. This is discussed in Appendix F.2.

We find similar results in the Bipedal Soccer task, shown in Figure 3b. For this task in particular the goal space is large making it difficult for HIRO to learn efficiently. Our method is able to outperform HIRO by completing the task in only half the number of environment steps. We also find that HAC was not able to solve the task and is not shown.

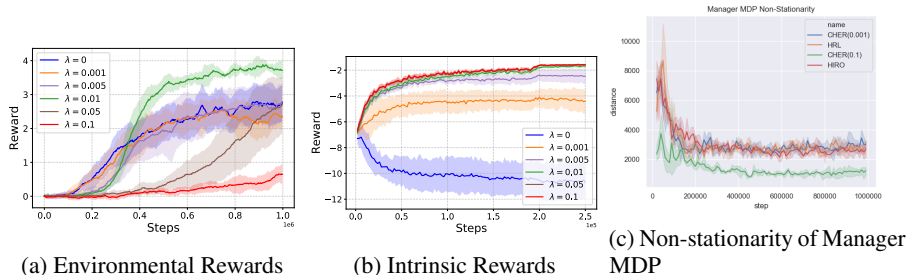


Figure 5: Effect of choice of λ .

The improvements in environmental returns in all tasks are equally coupled with a set of improvements in the intrinsic returns as seen in Figure 5, thereby validating the ability of the CHER algorithm to improve cooperation between the two policies.

5.4 Cooperation Tradeoff

In this section, we explore the effects and implications of using different values of λ for the connected-gradient weight. Fig. 5 depicts the effect of the choice of λ on the performance of both the manager and worker policies in the Ant Gather environment. When the value of λ equals 0, the algorithm is akin to the naive goal-conditioned HRL scheme as explained in Section 3.1. For small values of λ , we witness improvements in intrinsic rewards that do not result in noticeable changes to the performance of the training algorithm. As we increase the λ term, however, the increase in coordination begins to slow down improvements in environmental returns at the early stages of training. The corresponding increase in cooperation, however, results in a situation whereby the manager policy can confidently identify the effects of local goals on the actions the worker performs, ultimately allowing the overall policy to train much more efficiently. This initial slowing in training, however, begins to intensify for larger λ terms in which the values of the worker gradient send too strong of a signal to the manager policy, thereby slowing down or stopping training completely. Interestingly enough, this does not result in significant improvement in the intrinsic returns from the most high-performing λ term. These results suggest that moderate values of λ are adequate to yield optimal results.

5.5 Effects on non-stationarity

To increase the robustness of HRL methods that train multiple levels at the same time it would be beneficial to understand and limit the amount of *non-stationarity* experienced by higher layers. Here we perform a version of the analysis from the view of the manager policy. We perform an examination of how much the worker policy distribution changes under the manager. The more this distribution changes the more variance that is introduced into the managers reward estimates. We find that the CHER limits the amount of non-stationarity experienced by the manager and it appears to be a function of the λ term. We show this comparison in Fig.5c where we can see that CHER achieves lower divergence and therefore lower non-stationarity issues. These reductions can be a partial indication as to why CHER performs better than other methods compared to in this paper. In Appendix B we provide some mathematical motivation for why CHER can reduce non-stationarity.

6 Conclusions and future work

In this work, we propose connections between multi agent and hierarchical reinforcement learning that motivates our novel method of inducing cooperation in hierarchies. We provide a derivation of the gradient of a manager policy with respect to its workers for an actor-critic formulation as well as introducing a λ weighting term for this gradient which controls the level of cooperation. We find that using CHER results in consistently better-performing policies, that have lower empirical non-stationarity than prior work, particularly for more difficult tasks.

For future work, we would like to expand our framework of inter-level cooperation to support the accelerated training of stochastic policies, as is the case in the PPO [35] and SAC [33] algorithms, as

well as extend the cooperative HRL formulation to multi-level hierarchies, in which the multi-agent nature of hierarchical training is likely to be increasingly detrimental to training performance. We also hope to adapt insights from the effects of choice of cooperative weighting parameter to design adaptive methods for assigning the λ term as training progresses.

Broader Impacts

In this work we investigate new methods to enable policy learning via additional communication in multi-level control schemes. We are motivated by recent work in multi agent learning and biological control structures. These multi-level control schemes allow systems to be more modularized. This modularization allows us to break challenging control problems down into their smaller pieces. However, separation complicated the mathematical process used to train the agent. Our new connected gradient method allow high-level controllers to make decisions considering the capabilities of lower levels.

This work has the potential to broaden the applicability of recent RL methods to more difficult control problems. This may allow us to replace current heavily engineered methods with learned methods. For example, robot navigation platforms or even pathfinding schemes in video games. As the strength of these methods go it should allow people to focus on solving more complex tasks that were unrealizable before. For example, automated driving.

While these methods do not generally impose societal issues they can be used to solve problems that we may not want solved. While the authors are motivated to create methods to enable robots for societal good the methods could be used in weapons. We support the strong regulation of methods of this type when used in the world.

References

- [1] T. D. Kulkarni, K. Narasimhan, A. Saeedi, and J. Tenenbaum, "Hierarchical deep reinforcement learning: Integrating temporal abstraction and intrinsic motivation," in *Advances in neural information processing systems*, 2016, pp. 3675–3683.
- [2] C. Florensa, Y. Duan, and P. Abbeel, "Stochastic neural networks for hierarchical reinforcement learning," *arxiv preprint arxiv:1704.03012*, 2017.
- [3] O. Nachum, S. S. Gu, H. Lee, and S. Levine, "Data-efficient hierarchical reinforcement learning," in *Advances in Neural Information Processing Systems*, 2018, pp. 3303–3313.
- [4] P. Dayan and G. E. Hinton, "Feudal reinforcement learning," in *Advances in neural information processing systems*, 1993, pp. 271–278.
- [5] A. S. Vezhnevets, S. Osindero, T. Schaul, N. Heess, M. Jaderberg, D. Silver, and K. Kavukcuoglu, "Feudal networks for hierarchical reinforcement learning," *arXiv preprint arXiv:1703.01161*, 2017.
- [6] A. Levy, R. Platt, and K. Saenko, "Hierarchical actor-critic," *arXiv preprint arXiv:1712.00948*, 2017.
- [7] J. Hu and M. P. Wellman, "Nash q-learning for general-sum stochastic games," *Journal of machine learning research*, vol. 4, no. Nov, pp. 1039–1069, 2003.
- [8] D. Srinivasan, *Innovations in Multi-Agent Systems and Application-1*. Springer, 2010, vol. 310.
- [9] L. Matignon, G. J. Laurent, and N. Le Fort-Piat, "Independent reinforcement learners in cooperative markov games: a survey regarding coordination problems," *The Knowledge Engineering Review*, vol. 27, no. 1, pp. 1–31, 2012.
- [10] P. Hernandez-Leal, B. Kartal, and M. E. Taylor, "A survey and critique of multiagent deep reinforcement learning," *Autonomous Agents and Multi-Agent Systems*, vol. 33, no. 6, pp. 750–797, 2019.
- [11] T. T. Nguyen, N. D. Nguyen, and S. Nahavandi, "Deep reinforcement learning for multiagent systems: A review of challenges, solutions, and applications," *IEEE transactions on cybernetics*, 2020.
- [12] L. Busoniu, R. Babuska, and B. De Schutter, "Multi-agent reinforcement learning: A survey," in *2006 9th International Conference on Control, Automation, Robotics and Vision*. IEEE, 2006, pp. 1–6.
- [13] M. Weinberg and J. S. Rosenschein, "Best-response multiagent learning in non-stationary environments," in *Proceedings of the Third International Joint Conference on Autonomous Agents and Multiagent Systems-Volume 2*. IEEE Computer Society, 2004, pp. 506–513.
- [14] J. Foerster, N. Nardelli, G. Farquhar, T. Afouras, P. H. Torr, P. Kohli, and S. Whiteson, "Stabilising experience replay for deep multi-agent reinforcement learning," *arXiv preprint arXiv:1702.08887*, 2017.
- [15] A. Tampuu, T. Matiisen, D. Kodelja, I. Kuzovkin, K. Korjus, J. Aru, J. Aru, and R. Vicente, "Multiagent cooperation and competition with deep reinforcement learning," *PloS one*, vol. 12, no. 4, p. e0172395, 2017.
- [16] C. Claus and C. Boutilier, "The dynamics of reinforcement learning in cooperative multiagent systems," *AAAI/IAAI*, vol. 1998, no. 746-752, p. 2, 1998.

- [17] M. Tan, “Multi-agent reinforcement learning: Independent vs. cooperative agents,” in *Proceedings of the tenth international conference on machine learning*, 1993, pp. 330–337.
- [18] M. J. Hausknecht, “Cooperation and communication in multiagent deep reinforcement learning,” Ph.D. dissertation, University of Texas at Austin, 2016.
- [19] I. Mordatch and P. Abbeel, “Emergence of grounded compositional language in multi-agent populations,” in *Thirty-Second AAAI Conference on Artificial Intelligence*, 2018.
- [20] T. Eccles, Y. Bachrach, G. Lever, A. Lazaridou, and T. Graepel, “Biases for emergent communication in multi-agent reinforcement learning,” in *Advances in Neural Information Processing Systems*, 2019, pp. 13 111–13 121.
- [21] S. Sukhbaatar, A. Szlam, and R. Fergus, “Learning multiagent communication with backpropagation,” *CoRR*, vol. abs/1605.07736, 2016. [Online]. Available: <http://arxiv.org/abs/1605.07736>
- [22] J. N. Foerster, Y. M. Assael, N. de Freitas, and S. Whiteson, “Learning to communicate with deep multi-agent reinforcement learning,” *CoRR*, vol. abs/1605.06676, 2016. [Online]. Available: <http://arxiv.org/abs/1605.06676>
- [23] L. Panait and S. Luke, “Cooperative multi-agent learning: The state of the art,” *Autonomous agents and multi-agent systems*, vol. 11, no. 3, pp. 387–434, 2005.
- [24] R. Bellman, “A markovian decision process,” *Journal of Mathematics and Mechanics*, pp. 679–684, 1957.
- [25] R. S. Sutton, D. Precup, and S. Singh, “Between mdps and semi-mdps: A framework for temporal abstraction in reinforcement learning,” *Artificial intelligence*, vol. 112, no. 1-2, pp. 181–211, 1999.
- [26] R. Parr and S. J. Russell, “Reinforcement learning with hierarchies of machines,” in *Advances in neural information processing systems*, 1998, pp. 1043–1049.
- [27] T. G. Dietterich, “Hierarchical reinforcement learning with the maxq value function decomposition,” *Journal of Artificial Intelligence Research*, vol. 13, pp. 227–303, 2000.
- [28] —, “The maxq method for hierarchical reinforcement learning,” in *In Proceedings of the Fifteenth International Conference on Machine Learning*. Morgan Kaufmann, 1998, pp. 118–126.
- [29] V. Mnih, K. Kavukcuoglu, D. Silver, A. A. Rusu, J. Veness, M. G. Bellemare, A. Graves, M. Riedmiller, A. K. Fidjeland, G. Ostrovski *et al.*, “Human-level control through deep reinforcement learning,” *Nature*, vol. 518, no. 7540, p. 529, 2015.
- [30] D. Silver, G. Lever, N. Heess, T. Degris, D. Wierstra, and M. Riedmiller, “Deterministic policy gradient algorithms,” in *ICML*, 2014.
- [31] O. Nachum, S. Gu, H. Lee, and S. Levine, “Near-optimal representation learning for hierarchical reinforcement learning,” *arXiv preprint arXiv:1810.01257*, 2018.
- [32] R. J. Williams, “Simple statistical gradient-following algorithms for connectionist reinforcement learning,” *Machine learning*, vol. 8, no. 3-4, pp. 229–256, 1992.
- [33] T. Haarnoja, A. Zhou, P. Abbeel, and S. Levine, “Soft actor-critic: Off-policy maximum entropy deep reinforcement learning with a stochastic actor,” *arXiv preprint arXiv:1801.01290*, 2018.
- [34] J. Schulman, S. Levine, P. Abbeel, M. Jordan, and P. Moritz, “Trust region policy optimization,” in *International conference on machine learning*, 2015, pp. 1889–1897.
- [35] J. Schulman, F. Wolski, P. Dhariwal, A. Radford, and O. Klimov, “Proximal policy optimization algorithms,” *arXiv preprint arXiv:1707.06347*, 2017.
- [36] J. Achiam, D. Held, A. Tamar, and P. Abbeel, “Constrained policy optimization,” in *Proceedings of the 34th International Conference on Machine Learning-Volume 70*. JMLR. org, 2017, pp. 22–31.
- [37] P. S. Thomas and A. G. Barto, “Conjugate markov decision processes,” in *Proceedings of the 28th International Conference on International Conference on Machine Learning*, 2011, pp. 137–144.
- [38] P. S. Thomas, “Policy gradient coagent networks,” in *Advances in Neural Information Processing Systems*, 2011, pp. 1944–1952.
- [39] G. Berseth, X. B. Peng, and M. van de Panne, “Terrain RL simulator,” *CoRR*, vol. abs/1804.06424, 2018. [Online]. Available: <http://arxiv.org/abs/1804.06424>
- [40] S. Fujimoto, H. van Hoof, and D. Meger, “Addressing function approximation error in actor-critic methods,” *arXiv preprint arXiv:1802.09477*, 2018.
- [41] T. P. Lillicrap, J. J. Hunt, A. Pritzel, N. Heess, T. Erez, Y. Tassa, D. Silver, and D. Wierstra, “Continuous control with deep reinforcement learning,” *arXiv preprint arXiv:1509.02971*, 2015.
- [42] R. Lowe, Y. Wu, A. Tamar, J. Harb, O. P. Abbeel, and I. Mordatch, “Multi-agent actor-critic for mixed cooperative-competitive environments,” in *Advances in Neural Information Processing Systems*, 2017, pp. 6379–6390.

- [43] E. Todorov, T. Erez, and Y. Tassa, "Mujoco: A physics engine for model-based control," in *2012 IEEE/RSJ International Conference on Intelligent Robots and Systems*. IEEE, 2012, pp. 5026–5033.
- [44] G. Berseth, X. B. Peng, and M. van de Panne, "Terrain rl simulator," *arXiv preprint arXiv:1804.06424*, 2018.
- [45] C. Wu, A. Kreidieh, K. Parvate, E. Vinitzky, and A. M. Bayen, "Flow: Architecture and benchmarking for reinforcement learning in traffic control," *arXiv preprint arXiv:1710.05465*, 2017.

A Derivation of cooperative manager gradients

In this section, we derive an analytic expression of the gradient of the manager policy in a two-level goal-conditioned hierarchy with respect to both the losses associated with the high level and low level policies. In mathematical terms, we are trying to derive an expression for the weighted summation of the derivation of both losses, expressed as follows:

$$\nabla_{\theta_m} \eta'_m = \nabla_{\theta_m} (\eta_m + \lambda \eta_w) = \nabla_{\theta_m} \eta_m + \lambda \nabla_{\theta_m} \eta_w \quad (7)$$

where λ is a weighting term and η_m and η_w are the expected returns assigned to the manager and worker policies, respectively. More specifically, these two terms are:

$$\eta_m = \mathbb{E}_{s \sim p_\pi} \left[\sum_{t=0}^{T/k} [\gamma^t (r_m(s_{kt}, \pi_m(s_{kt})))] \right] = \int_{\mathcal{S}} \rho_0(s) V_m(s) ds_t \quad (8)$$

$$\eta_w = \mathbb{E}_{s \sim p_\pi} \left[\sum_{t=0}^k \gamma^t r_w(s_t, g_t, \pi_w(s_t, g_t)) \right] = \int_{\mathcal{S}} \rho_0(s) V_w(s_t, g_t) ds_t \quad (9)$$

Here, under the actor-critic formulation we replace the expected return under a given starting state with the value functions V_m and V_w . This is integrated over the distribution of initial states $\rho_0(\cdot)$.

Following the results by [30], we can express the first term in Eq. (6) as:

$$\nabla_{\theta_m} \eta_m = \mathbb{E}_{s \sim p_\pi} [\nabla_a Q_m(s, a)|_{a=\pi_m(s)} \nabla_{\theta_m} \pi_m(s)] \quad (10)$$

We now expand the second term of the gradient into a function of the manager and worker actor (π_m, π_w) and critic (Q_m, Q_w) policies and their trainable parameters. In order to propagate the loss associated with the worker through the policy parameters of the manager, we assume that the goals assigned to the worker g_t are not fixed variables, but rather temporally abstracted outputs from the manager policy π_m , and may be updated in between decisions by the manager via a transition function h . Mathematically, the goal transition is defined as:

$$g_t(\theta_m) = \begin{cases} \pi_m(s_t) & \text{if } t \bmod k = 0 \\ h(s_{t-1}, g_{t-1}(\theta_m), s_t) & \text{otherwise} \end{cases} \quad (11)$$

For the purposes of simplicity, we express the manager output term as g_t from now on.

We begin by computing the partial derivative of the worker value function with respect to the parameters of the manager:

$$\begin{aligned} \nabla_{\theta_m} V_w(s_t, g_t) &= \nabla_{\theta_m} Q_w(s_t, g_t, \pi_w(s_t, g_t)) \\ &= \nabla_{\theta_m} \left(r_w(s_t, g_t, \pi_w(s_t, g_t)) + \int_{\mathcal{G}} \int_{\mathcal{S}} \gamma p_w(s', g' | s_t, g_t, \pi_w(s_t, g_t)) V_w(s', g') ds' dg' \right) \\ &= \nabla_{\theta_m} r_w(s_t, g_t, \pi_w(s_t, g_t)) + \gamma \nabla_{\theta_m} \int_{\mathcal{G}} \int_{\mathcal{S}} p_w(s', g' | s_t, g_t, \pi_w(s_t, g_t)) V_w(s', g') ds' dg' \end{aligned} \quad (12)$$

where \mathcal{G} and \mathcal{S} are the goal and environment state spaces, respectively, and $p_w(\cdot, \cdot | \cdot, \cdot, \cdot)$ is the probability distribution of the next state from the perspective of the worker given the current state and action.

Expanding the latter term, we get:

$$p_w(s', g' | s_t, g_t, \pi_w(s_t, g_t)) = p_{w,1}(g' | s', s_t, g_t, \pi_w(s_t, g_t)) p_{w,2}(s' | s_t, g_t, \pi_w(s_t, g_t)) \quad (13)$$

The first element, $p_{w,1}$, is the probability distribution of the next goal, and is deterministic with respect to the conditional variables. Specifically:

$$p_{w,1}(g' | s_t, g_t, \pi_w(s_t, g_t)) = \begin{cases} 1 & \text{if } g' = g_{t+1} \\ 0 & \text{otherwise} \end{cases} \quad (14)$$

The second element, $p_{w,2}$, is the state transition probability from the MDP formulation of the task, i.e.

$$p_{w,2}(s' | s_t, g_t, \pi_w(s_t, g_t)) = p(s' | s_t, \pi_w(s_t, g_t)) \quad (15)$$

Combining Eq. (13)-(15) into Eq. (12), we get:

$$\begin{aligned}
\nabla_{\theta_m} V_w(s_t, g_t) &= \nabla_{\theta_m} r_w(s_t, g_t, \pi_w(s_t, g_t)) \\
&\quad + \gamma \nabla_{\theta_m} \int_{\mathcal{G}} \int_{\mathcal{S}} \left(p_{w,1}(g'|s', s_t, g_t, \pi_w(s_t, g_t)) p_{w,2}(s'|s_t, g_t, \pi_w(s_t, g_t)) V_w(s', g') ds' dg' \right) \\
&= \nabla_{\theta_m} r_w(s_t, g_t, \pi_w(s_t, g_t)) \\
&\quad + \gamma \nabla_{\theta_m} \int_{\mathcal{G} \cap \{g_{t+1}\}} \int_{\mathcal{S}} 1 \cdot p(s'|s_t, \pi_w(s_t, g_t)) V_w(s', g') ds' dg' \\
&\quad + \gamma \nabla_{\theta_m} \int_{(\mathcal{G} \cap \{g_{t+1}\})^c} \int_{\mathcal{S}} 0 \cdot p(s'|s_t, \pi_w(s_t, g_t)) V_w(s', g') ds' dg' \\
&= \nabla_{\theta_m} r_w(s_t, g_t, \pi_w(s_t, g_t)) + \gamma \nabla_{\theta_m} \int_{\mathcal{S}} p(s'|s_t, \pi_w(s_t, g_t)) V_w(s', g_{t+1}) ds'
\end{aligned} \tag{16}$$

Continuing the derivation of $\nabla_{\theta_m} V_w$ from Eq. (16), we get,

$$\begin{aligned}
\nabla_{\theta_m} V_w(s_t, g_t) &= \nabla_{\theta_m} r_w(s_t, g_t, \pi_w(s_t, g_t)) + \gamma \nabla_{\theta_m} \int_{\mathcal{S}} p(s'|s_t, \pi_w(s_t, g_t)) V_w(g_{t+1}, s') ds' \\
&= \nabla_{\theta_m} r_w(s_t, g_t, \pi_w(s_t, g_t)) + \gamma \int_{\mathcal{S}} \nabla_{\theta_m} p(s'|s_t, \pi_w(s_t, g_t)) V_w(g_{t+1}, s') ds' \\
&= \nabla_{\theta_m} g_t \nabla_g r_w(s_t, g, \pi_w(s_t, g_t)) \Big|_{g=g_t} \\
&\quad + \nabla_{\theta_m} g_t \nabla_g \pi_w(s_t, g) \Big|_{g=g_t} \nabla_a r_w(s_t, g_t, a) \Big|_{a=\pi_w(s_t, g_t)} \\
&\quad + \gamma \int_{\mathcal{S}} \left(V_w(s', g_{t+1}) \nabla_{\theta_m} g_t \nabla_g \pi_w(s_t, g) \Big|_{g=g_t} \nabla_a p(s'|s_t, a) \Big|_{a=\pi_w(s_t, g_t)} ds' \right) \\
&\quad + \gamma \int_{\mathcal{S}} p(s'|s_t, \pi_w(s_t, g_t)) \nabla_{\theta_m} V_w(s', g_{t+1}) ds' \\
&= \nabla_{\theta_m} g_t \nabla_g \left(r_w(s_t, g, \pi_w(s_t, g_t)) \right. \\
&\quad \quad \quad + \pi_w(s_t, g) \nabla_a r_w(s_t, g_t, a) \Big|_{a=\pi_w(s_t, g_t)} \\
&\quad \quad \quad \left. + \gamma \int_{\mathcal{S}} V_w(s', g_{t+1}) \pi_w(s_t, g) \nabla_a p(s'|s_t, a) \Big|_{a=\pi_w(s_t, g_t)} ds' \right) \Big|_{g=g_t} \\
&\quad + \gamma \int_{\mathcal{S}} p(s'|s_t, \pi_w(s_t, g_t)) \nabla_{\theta_m} V_w(s', g_{t+1}) ds' \\
&= \nabla_{\theta_m} g_t \nabla_g \left(r_w(s_t, g, \pi_w(s_t, g_t)) \right. \\
&\quad \quad \quad \left. + \pi_w(s_t, g) \nabla_a \left(r_w(s_t, g_t, a) + \gamma \int_{\mathcal{S}} V_w(s', g_{t+1}) p(s'|s_t, a) ds' \right) \Big|_{a=\pi_w(s_t, g_t)} \right) \Big|_{g=g_t} \\
&\quad + \gamma \int_{\mathcal{S}} p(s'|s_t, \pi_w(s_t, g_t)) \nabla_{\theta_m} V_w(s', g_{t+1}) ds' \\
&= \nabla_{\theta_m} g_t \nabla_g \left(r_w(s_t, g, \pi_w(s_t, g_t)) + \pi_w(s_t, g) \nabla_a Q_w(s_t, g_t, a) \Big|_{a=\pi_w(s_t, g_t)} \right) \Big|_{g=g_t} \\
&\quad + \gamma \int_{\mathcal{S}} p(s'|s_t, \pi_w(s_t, g_t)) \nabla_{\theta_m} V_w(s', g_{t+1}) ds'
\end{aligned} \tag{17}$$

Iterating this formula, we have,

$$\begin{aligned}
\nabla_{\theta_m} V_w(s_t, g_t) &= \nabla_{\theta_m} g_t \nabla_g \left(r_w(s_t, g, \pi_w(s_t, g_t)) + \pi_w(s_t, g) \nabla_a Q_w(s_t, g_t, a) \Big|_{a=\pi_w(s_t, g_t)} \right) \Big|_{g=g_t} \\
&\quad + \gamma \int_{\mathcal{S}} p(s_{t+1}|s_t, \pi_w(s_t, g_t)) \nabla_{\theta_m} V_w(s_{t+1}, g_{t+1}) ds_{t+1} \\
&= \nabla_{\theta_m} g_t \nabla_g \left(r_w(s_t, g, \pi_w(s_t, g_t)) + \pi_w(s_t, g) \nabla_a Q_w(s_t, g_t, a) \Big|_{a=\pi_w(s_t, g_t)} \right) \Big|_{g=g_t} \\
&\quad + \gamma \int_{\mathcal{S}} p(s_{t+1}|s_t, \pi_w(s_t, g_t)) \nabla_{\theta_m} g_{t+1} \nabla_g \left(r_w(s_{t+1}, g, \pi_w(s_{t+1}, g_{t+1})) \right. \\
&\quad \quad \left. + \pi_w(s_{t+1}, g) \nabla_a Q_w(s_{t+1}, g_{t+1}, a) \Big|_{a=\pi_w(s_{t+1}, g_{t+1})} \right) \Big|_{g=g_{t+1}} ds_{t+1} \\
&\quad + \gamma^2 \int_{\mathcal{S}} \int_{\mathcal{S}} \left(p(s_{t+1}|s_t, \pi_w(s_t, g_t)) p(s_{t+2}|s_{t+1}, \pi_w(g_{t+1}, s_{t+1})) \right. \\
&\quad \quad \left. \nabla_{\theta_m} V_w(s_{t+2}, g_{t+2}) ds_{t+2} ds_{t+1} \right) \\
&\quad \quad \quad \vdots \\
&= \sum_{n=0}^{\infty} \gamma^n \underbrace{\int_{\mathcal{S}} \cdots \int_{\mathcal{S}}}_{n \text{ times}} \left(\prod_{k=0}^{n-1} p(s_{t+k+1}|s_{t+k}, \pi_w(s_{t+k}, g_{t+k})) \right) \\
&\quad \quad \times \nabla_{\theta_m} g_{t+n} \nabla_g \left(r_w(s_{t+n}, g, \pi_w(s_{t+n}, g_{t+n})) \right. \\
&\quad \quad \left. + \pi_w(s_{t+n}, g) \nabla_a Q_w(s_{t+n}, g_{t+n}, a) \Big|_{a=\pi_w(s_{t+n}, g_{t+n})} \right) \Big|_{g=g_{t+n}} ds_{t+n} \cdots ds_{t+1}
\end{aligned} \tag{18}$$

Taking the gradient of the expected worker value function, we get,

$$\begin{aligned}
\nabla_{\theta_m} \eta_w &= \nabla_{\theta_m} \int_{\mathcal{S}} \rho_0(s_0) V_w(s_0, g_0) ds_0 \\
&= \int_{\mathcal{S}} \rho_0(s_0) \nabla_{\theta_m} V_w(s_0, g_0) ds_0 \\
&= \int_{\mathcal{S}} \rho_0(s_0) \sum_{n=0}^{\infty} \gamma^n \underbrace{\int_{\mathcal{S}} \cdots \int_{\mathcal{S}}}_{n \text{ times}} \left[\left(\prod_{k=0}^{n-1} p(s_{k+1}|s_k, \pi_w(s_k, g_k)) \right) \nabla_{\theta_m} g_n \right. \\
&\quad \quad \left. \times \nabla_g \left(r_w(s_n, g, \pi_w(s_n, g_n)) + \pi_w(s_n, g) \nabla_a Q_w(s_n, g_n, a) \Big|_{a=\pi_w(s_n, g_n)} \right) \right] \Big|_{g=g_n} ds_n \cdots ds_0 \tag{19} \\
&= \sum_{n=0}^{\infty} \underbrace{\int_{\mathcal{S}} \cdots \int_{\mathcal{S}}}_{n+1 \text{ times}} \gamma^n p_{\theta_m, \theta_w, n}(\tau) \nabla_{\theta_m} g_n \nabla_g \left(r_w(s_n, g, \pi_w(s_n, g_n)) \right. \\
&\quad \quad \left. + \pi_w(s_n, g) \nabla_a Q_w(s_n, g_n, a) \Big|_{a=\pi_w(s_n, g_n)} \right) \Big|_{g=g_n} ds_n \cdots ds_0 \\
&= \mathbb{E}_{\tau \sim p_{\theta_m, \theta_w}} \left[\nabla_{\theta_m} g_t \nabla_g \left(r_w(s_t, g, \pi_w(s_t, g_t)) + \pi_w(s_t, g) \nabla_a Q_w(s_t, g_t, a) \Big|_{a=\pi_w(s_t, g_t)} \right) \Big|_{g=g_t} \right]
\end{aligned}$$

where $\tau = (s_0, a_0, s_1, a_1, \dots, s_n)$ is a trajectory and $p_{\theta_m, \theta_w, n}(\tau)$ is the (improper) discounted probability of witnessing a trajectory a set of policy parameters θ_m and θ_w .

The final representation of the connected gradient formulation is then:

$$\begin{aligned}
\nabla_{\theta_m} \eta'_m &= \mathbb{E}_{s \sim p_{\pi}} \left[\nabla_a Q_m(s, a) \Big|_{a=\pi_m(s)} \nabla_{\theta_m} \pi_m(s) \right] \\
&\quad + \mathbb{E}_{\tau \sim p_{\theta_m, \theta_w}(\tau)} \left[\nabla_{\theta_m} g_t \nabla_g \left(r_w(s_t, g, \pi_w(s_t, g_t)) + \pi_w(s_t, g) \nabla_a Q_w(s_t, g_t, a) \Big|_{a=\pi_w(s_t, g_t)} \right) \Big|_{g=g_t} \right] \tag{20}
\end{aligned}$$

B Non-stationarity in hierarchical reinforcement learning

In multi-agent RL, several independent agents interact with an environment as well as one another. In this setting, the MDP of any individual agent i is:

$$\text{MDP}_i = (\mathcal{S}_i, \mathcal{A}_i, \mathcal{P}_i, r_i, \rho_{0,i}, \gamma, T, \pi_{\theta}^{-i}) \tag{21}$$

where, in addition to the variables depicted in Section 2.1, the environment is further characterized by the policies of all other agents within the network π_{θ}^{-i} , which evolve as training progresses. These additional evolving terms contribute to the nonstationarity of the environment from the perspective of a particular agent since it is always changing, a factor that can be seen as invalidating the use of standard off-policy temporal difference learning in multi-agent settings [42]. Similarly, in the hierarchical model architecture depicted in Section 2.2, it can be seen that the manager and worker policies, π_m and π_w , exist under similar environmental settings as those experienced in multi-agent systems, with the MDP of each policy expressed as:

$$\text{MDP}_m = (\mathcal{S}, \mathcal{A}_m, \mathcal{P}, r_m, \rho_0, \gamma, T/k, \pi_w), \quad \text{MDP}_w = (\mathcal{S}, \mathcal{A}_w, \mathcal{P}, r_w, \rho_0, \gamma, k, \pi_m) \quad (22)$$

As a result, the aforementioned non-stationarity effects of off-policy training in multi-agent reinforcement learning (MARL) are a potential limiting factor in HRL as well, due to each policy constantly changing from the perspective of the other.

B.1 Connecting non-stationarity to the worker policy

In this section we introduce a method to understand the non-stationarity of the learning problem from the point of view of the manager policy. Without sufficiently small amount of non-stationarity the manager policy will not be able to learn a good policy as a result of having an MDP where it is too difficult to estimate transition dynamics. Therefore we introduce analysis and a bound on the manager’s non-stationarity as a function of the change in the worker policy.

Definition 1. *Meta period.* We write the meta period as an integer k .

Definition 2. *Training iteration.* We write the training iteration as an integer i .

Definition 3. *Transition probabilities.* Define the symbol $p(t)$ to be equal to the transition probabilities $p(s_{t+1}|s_t, a_t)$ of entering a particular state s_{t+1} at time step t .

Definition 4. *Action probabilities.* Define the symbol $\pi_{l_o}^{(i)}(t)$ to be the action probabilities $\pi_{l_o}^{(i)}(a_t|s_t, g_t)$ of taking an action a_t at training iteration i and time step t .

Definition 5. *Non-stationarity.* We write non-stationarity as the total variation distance between sequential iterations i of the high level transition dynamics.

$$d_{ns} = \sup_{s_t, g_t} \mathcal{D}_{TV} \left(p^{(i+1)}(s_{t+k}|s_t, g_t) \parallel p^{(i)}(s_{t+k}|s_t, g_t) \right) \quad (23)$$

Assumption 1. *Boundedness of transition probabilities.* We assume that $\forall s_{t+1}, \forall s_t, \forall a_t$ the transition probabilities are upper bounded by a finite c , such that $p(s_{t+1}|s_t, a_t) \leq c$.

Assumption 2. *Boundedness of action probabilities.* We assume that $\forall a_t, \forall s_t, \forall g_t$ the action probabilities are upper bounded by a finite b and lower bounded by a non-zero f , such that $f \leq \pi_{l_o}^{(i+1)}(s_{t+1}|s_t, a_t) \leq b$.

Theorem 2. *If the Kullback–Leibler divergence of worker policies at different training iterations is upper bounded by ϵ , then we have a bound on non-stationarity.*

$$\sup_{s_t, g_t} \mathcal{D}_{KL} \left(\pi_{l_o}^{(i+1)}(a_t|s_t, g_t) \parallel \pi_{l_o}^{(i)}(a_t|s_t, g_t) \right) \leq \epsilon \implies d_{ns} \leq \sqrt{2k\epsilon} \left(\frac{b\sqrt{c}}{f} \right)^{2k} \quad (24)$$

Proof. We begin this proof by writing the state-goal transition dynamics in terms of lower level actions using the marginalization property of probability.

$$p^{(i+1)}(s_{t+k}|s_t, g_t) = \mathbb{E}_{\pi_{l_o}^{(i+1)}} \left[p^{(i+1)}(s_{t+k}, \dots, s_{t+1}, a_{t+k-1}, \dots, a_t|s_t, g_t) \right] \quad (25)$$

We define K as a particular product.

$$K = p(t+k) \prod_{j=0}^{k-1} p(t+j) \quad (26)$$

This allows a simplified expression for the transition dynamics at iteration $i + 1$.

$$p^{(i+1)}(s_{t+k}|s_t, g_t) = \mathbb{E}_{\pi_{l_o}^{(i+1)}} \left[K \prod_{j=0}^{k-1} \pi_{l_o}^{(i+1)}(t+j) \right] \quad (27)$$

We can also express the transition dynamics at iteration i in terms of samples drawn from the lower level policy at iteration $i + 1$ using importance sampling of the actions a_t .

$$p^{(i)}(s_{t+k}|s_t, g_t) = \mathbb{E}_{\pi_{l_o}^{(i+1)}} \left[K \prod_{j=0}^{k-1} \frac{\pi_{l_o}^{(i)}(t+j)^2}{\pi_{l_o}^{(i+1)}(t+j)} \right] \quad (28)$$

Using the definition for the total variation distance, we can write the non-stationary distribution change d_{ns} in terms of an absolute difference between transition dynamics at training iterations $i + 1$ and i .

$$d_{ns} = \sup_{s_{t+k}, s_t, g_t} \left| p^{(i+1)}(s_{t+k}|s_t, g_t) - p^{(i)}(s_{t+k}|s_t, g_t) \right| \quad (29)$$

We first replace the transition dynamics with their expanded forms using the results in equation 27 and 28.

$$d_{ns} = \sup_{s_{t+k}, s_t, g_t} \left| \mathbb{E}_{\pi_{l_o}^{(i+1)}} \left[K \prod_{j=0}^{k-1} \pi_{l_o}^{(i+1)}(t+j) - K \prod_{j=0}^{k-1} \frac{\pi_{l_o}^{(i)}(t+j)^2}{\pi_{l_o}^{(i+1)}(t+j)} \right] \right| \quad (30)$$

We remove K . We do so by introducing a bound on the maximum value for K , namely K_{\max} .

$$K_{\max} = \sup_{s_t, \dots, s_{t+k}, a_t, \dots, a_{t+k}} \left| p(t+k) \prod_{j=0}^{k-1} p(t+j) \right| \quad (31)$$

Assuming boundedness in Assumption 1, K_{\max} is upper bounded by c^k .

$$K_{\max} \leq c^k \quad (32)$$

We replace K with its upper bound, and pull that common factor outside of the expected value and the norm. This results in a bound on d_{ns} independent of the transition probabilities.

$$d_{ns} \leq c^k \sup_{s_{t+k}, s_t, g_t} \left| \mathbb{E}_{\pi_{l_o}^{(i+1)}} \left[\prod_{j=0}^{k-1} \pi_{l_o}^{(i+1)}(t+j) - \prod_{j=0}^{k-1} \frac{\pi_{l_o}^{(i)}(t+j)^2}{\pi_{l_o}^{(i+1)}(t+j)} \right] \right| \quad (33)$$

We then remove an extra factor of $\prod_{j=0}^{k-1} \pi_{l_o}^{(i+1)}(t+j)^2$. Likewise, we do this by introducing a bound on the maximum value of this distribution, namely Π_{\max} .

$$\Pi_{\max} = \sup_{s_t, \dots, s_{t+k}, a_t, \dots, a_{t+k}, g_t} \left| \prod_{j=0}^{k-1} \pi_{l_o}^{(i+1)}(t+j) \right| \quad (34)$$

Assuming boundedness in Assumption 2, Π_{\max} is upper bounded by b^k .

$$\Pi_{\max} \leq b^k \quad (35)$$

We replace the extra factor of $\prod_{j=0}^{k-1} \pi_{l_o}^{(i+1)}(t+j)^2$ with its upper bound, and pull that common factor outside of the expected value and the norm. This results in a another simplified upper bound on d_{ns} .

$$d_{ns} \leq (bc)^k \sup_{s_{t+k}, s_t, g_t} \left| \mathbb{E}_{\pi_{l_o}^{(i+1)}} \left[1 - \prod_{j=0}^{k-1} \frac{\pi_{l_o}^{(i)}(t+j)^2}{\pi_{l_o}^{(i+1)}(t+j)^2} \right] \right| \quad (36)$$

In order to make the innermost terms of the expected value resemble a difference, we can factor out a surrogate reciprocal factor of $\prod_{j=0}^{k-1} \pi_{lo}^{(i+1)}(t+j)^2$. First, express the lower bound Π_{\min} .

$$\Pi_{\min} = \inf_{s_t, \dots, s_{t+k}, a_t, \dots, a_{t+k}, g_t} \left| \prod_{j=0}^{k-1} \pi_{lo}^{(i+1)}(t+j) \right| \quad (37)$$

Assuming boundedness in Assumption 2, Π_{\min} is lower bounded by f^k .

$$\pi_{lo}^{(i+1)}(t) \geq f \implies \Pi_{\min} \geq f^k \quad (38)$$

We factor out the reciprocal of $\prod_{j=0}^{k-1} \pi_{lo}^{(i+1)}(t+j)^2$.

$$d_{\text{ns}} \leq (bc)^k \sup_{s_{t+k}, s_t, g_t} \left| \mathbb{E}_{\pi_{lo}^{(i+1)}} \left[\prod_{j=0}^{k-1} \frac{1}{\pi_{lo}^{(i+1)}(t+j)^2} \left(\prod_{j=0}^{k-1} \pi_{lo}^{(i+1)}(t+j)^2 - \prod_{j=0}^{k-1} \pi_{lo}^{(i)}(t+j)^2 \right) \right] \right| \quad (39)$$

Then, replace that reciprocal with its upper bound, namely f^{-2k}

$$d_{\text{ns}} \leq \left(\frac{bc}{f^2} \right)^k \sup_{s_{t+k}, s_t, g_t} \left| \mathbb{E}_{\pi_{lo}^{(i+1)}} \left[\prod_{j=0}^{k-1} \pi_{lo}^{(i+1)}(t+j)^2 - \prod_{j=0}^{k-1} \pi_{lo}^{(i)}(t+j)^2 \right] \right| \quad (40)$$

Note an important property that follows with the assumptions that we have required at the beginning of this proof. The sum of joint lower level action distributions is upper bounded by $2b^k$.

$$\prod_{j=0}^{k-1} \pi_{lo}^{(i+1)}(t+j) + \prod_{j=0}^{k-1} \pi_{lo}^{(i)}(t+j) \leq 2b^k \quad (41)$$

We remove the squared operation, to arrive at an expression like total variation distance. We observe the difference of squares, and replace the positive factor with its upper bound, namely $2b^k$.

$$d_{\text{ns}} \leq 2 \left(\frac{b\sqrt{c}}{f} \right)^{2k} \sup_{s_{t+k}, s_t, g_t} \left| \mathbb{E}_{\pi_{lo}^{(i+1)}} \left[\prod_{j=0}^{k-1} \pi_{lo}^{(i+1)}(t+j) - \prod_{j=0}^{k-1} \pi_{lo}^{(i)}(t+j) \right] \right| \quad (42)$$

Finally, we can upper bound the expected value by taking the maximum over all possible assignments to the variables being sampled, namely the states s_t , actions a_t , and goals g_t .

$$d_{\text{ns}} \leq 2 \left(\frac{b\sqrt{c}}{f} \right)^{2k} \sup_{s_t, \dots, s_{t+k}, g_t, a_t, \dots, a_{t+k}} \left| \prod_{j=0}^{k-1} \pi_{lo}^{(i+1)}(t+j) - \prod_{j=0}^{k-1} \pi_{lo}^{(i)}(t+j) \right| \quad (43)$$

This is the form of a total variation distance.

$$d_{\text{ns}} \leq 2 \left(\frac{b\sqrt{c}}{f} \right)^{2k} \sup_{s_t, \dots, s_{t+k}, g_t} \mathcal{D}_{TV} \left(\prod_{j=0}^{k-1} \pi_{lo}^{(i+1)}(t+j) \left\| \prod_{j=0}^{k-1} \pi_{lo}^{(i)}(t+j) \right. \right) \quad (44)$$

We can replace that total variation distance with an upper bound. Note the divergence of two products of k factors can be expressed as the sum of k pairwise divergences.

$$d_{\text{ns}} \leq 2 \left(\frac{b\sqrt{c}}{f} \right)^{2k} \sup_{s_t, \dots, s_{t+k}, g_t} \sqrt{\frac{1}{2} \sum_{j=0}^{k-1} \mathcal{D}_{KL} \left(\pi_{lo}^{(i+1)}(t+j) \left\| \pi_{lo}^{(i)}(t+j) \right. \right)} \quad (45)$$

The final step is to replace that sum with k times its maximal value, taken over s_t , and g_t .

$$d_{\text{ns}} \leq 2 \left(\frac{b\sqrt{c}}{f} \right)^{2k} \sup_{s_t, g_t} \sqrt{\frac{k}{2} \mathcal{D}_{KL} \left(\pi_{l_o}^{(i+1)}(t) \parallel \pi_{l_o}^{(i)}(t) \right)} \quad (46)$$

We are given a bound on the Kullback–Leibler divergence at the beginning of the proof. We use this divergence bound to derive the final upper bound on the non-stationarity.

$$\sup_{s_t, g_t} \mathcal{D}_{KL} \left(\pi_{l_o}^{(i+1)}(t) \parallel \pi_{l_o}^{(i)}(t) \right) \leq \epsilon \implies d_{\text{ns}} \leq \sqrt{2k\epsilon} \left(\frac{b\sqrt{c}}{f} \right)^{2k} \quad (47)$$

We have established the implication at the beginning of the proof, which is a function of both the meta period and the bound variable ϵ on Kullback–Leibler divergence. \square

C CHER Algorithm

For completeness, we provide the CHER algorithm below.

Algorithm 1 CHER

```

1: Initialize policy parameters  $\theta_w, \theta_m$  and memory  $\mathcal{D}$ 
2: while True do g
3:   for each  $t = 0, \dots, T$  do
4:      $g_t \sim \pi_{\theta_m}(g_t | s_t)$  ▷ Sample manager action
5:      $a_t \sim \pi_{\theta_w}(a_t | s_t, g_t)$  ▷ Sample worker action
6:      $s_{t+1}, r_t^m \leftarrow \text{env.step}(a_t)$ 
7:      $r_t^w \leftarrow r_w(s_t, g_t, s_{t+1})$  ▷ Worker reward
8:   end for each
9:    $\theta_w \leftarrow \theta_w + \alpha \nabla_{\theta_w} \eta_w$  ▷ Train worker
10:   $\theta_m \leftarrow \theta_m + \alpha \nabla_{\theta_m} (\eta_m + \lambda \eta_w)$  ▷ Train manager
11: end while

```

D Environment details

D.1 Simulation details

The simulators and simulation horizons for each of the environments are as follows:

- The Ant Maze and Ant Gather environments are simulated using the MuJoCo physics engine for model-based control [43]. The time horizon in both tasks is set to 500 steps, with $dt = 0.02$ and $\text{frame skip} = 5$.
- The Bipedal Soccer environment using the TerrainRL simulator [44]. The time horizon for this task is set to 512 steps.
- The Single-Lane Highway environment is simulated using the Flow [45] computational framework for mixed autonomy traffic control with simulation step size of 0.4 seconds/step and frame skip of 3. The simulation is warmed up 500 steps (600 seconds) to allow for the downstream congested edge to generate regular and persistent stop-and-go wave before, and is controlled for 1500 steps (1800 seconds).

Finally, both the Ant Gather and Bipedal Soccer environments are terminated early if the agent falls/dies, defined as the z-coordinate of the agent being less than a certain threshold. If an agent dies, it receives a return of 0 for that time step.

D.2 Evaluation metrics

For all environments excluding the Ant Maze environment, results are reported over the average return from the past 100 episodes.

For the Ant Maze environment, during the training procedure, the agent is assigned (x, y) values between the range $(-4, -4) \times (20, 20)$ at the start of every episode. The performance of the agent is evaluated every 50,000 steps at the positions (16, 0), (16, 16), and (0, 16) based on a “success” metric, defined as achieved if the agent is within an L_2 distance of 5 from the target at the final step. This evaluation metric is averaged across 50 episodes.

E Algorithm details

E.1 Choice of hyperparamters

- Network shapes of (256, 256) for the actor and critic of both controllers with ReLU nonlinearities at the hidden layers and tanh nonlinearity at the output layer of the actors. The output of the actors are scaled to match the desired action space.
- Adam optimizer; learning rate: $3e-4$ for actor and critic of both controllers
- Soft update targets $\tau = 5e-3$ for both controllers
- Discount $\gamma = 0.99$ for both controllers.
- Replay buffer size: 200,000 for both controllers.
- Lower-level critic updates 1 environment step and delay actor and target critic updates every 2 steps.
- Higher-level critic updates 10 environment steps and delay actor and target critic updates every 20 steps.
- Huber loss function for the critic of both controllers.
- No gradient clipping.
- Exploration (for both controllers):
 - Initial purely random exploration for the first 10,000 time steps
 - Gaussian noise of the form $\mathcal{N}(0, 0.1 \times \text{action range})$ for all other steps
- Reward scale of 0.1 for Ant Maze, 10 for Ant Gather, and 1 for the bipedal/humanoid navigation and traffic control tasks.
- Number of candidate goals = 10^3
- Subgoal testing rate = 0.3^4
- Connected gradient weights λ are provided in the next sections.

E.2 Manager goal assignment

As mentioned in Section 5.2, the output layers of both the manager and worker policies are squashed by a tanh function and then scaled by the action space of the specific policy. The scaling terms for the worker policies in all environments are provided by the action space of the environment.

For the manager policy within the Ant Maze and Ant Gather environments, we follow the scaling terms utilized by [3]. The scaling term are accordingly ± 10 for the desired relative x, y ; ± 0.5 for the desired relative z ; ± 1 for the desired relative torso orientations; and the remaining limb angle ranges are available from the ant.xml file. More concretely, the action space of the higher-level policies are:

```
import gym
manager_action_space = gym.spaces.Box(
    low=[-10, -10, -0.5, -1, -1, -1, -1, -0.5, -0.3, -0.5, -0.3, -0.5, -0.3, -0.5, -0.3],
    high=[10, 10, 0.5, 1, 1, 1, 1, 0.5, 0.3, 0.5, 0.3, 0.5, 0.3, 0.5, 0.3]
)
```

For the manager policy within the Bipedal Soccer environment, we limit goal assignment to the root positions and velocities of the agent, as well as the orientation of the agent’s right and left feet. The scaling term are $[0, 1.5]$ for root height, ± 1 for the root pose, ± 2 for the positions of the right and left feet, $[\pm 2, \pm 1, \pm 2]$ in root velocity. The action space of the higher-level policy is accordingly:

```
manager_action_space = gym.spaces.Box(
    low=[0, -1, -1, -1, -1, -2, -2, -2, -2, -2, -2, -2, -1, -2],
    high=[1.5, 1, 1, 1, 1, 1, 2, 2, 2, 2, 2, 2, 1, 2]
)
```

³This hyperparameter is only used by the HIRO algorithm.

⁴This hyperparameter is only used by the HAC algorithm.

E.3 Worker intrinsic reward

We utilize an intrinsic reward function used for the worker that serves to characterize the goals as desired relative changes in observations, similar to [3]. The intrinsic reward function is accordingly:

$$r_w(s_t, g_t, s_{t+1}) = -\|s_t + g_t - s_{t+1}\|_2 \quad (48)$$

For the Bipedal Soccer environment, in which early terminations frequently occur as a result of the agent falling down, we offset this reward by the the largest possible distance measure in order to ensure that the rewards are always positive, thereby penalizing early terminations from the perspective of the worker policy. This intrinsic reward function is defined as:

$$r_w(s_t, g_t, s_{t+1}) = \|(g_{\max} - g_{\min})\|_2 - \|s_t + g_t - s_{t+1}\|_2 \quad (49)$$

where g_{\min} and g_{\max} are the goal-space low and high values, respectively.

Finally, in order to maintain the same absolute position of the goal regardless of state change, a goal-transition function $h(s_t, g_t, s_{t+1}) = s_t + g_t - s_{t+1}$ is used between goal-updates by the manager policy. The goal transition function is accordingly defined as:

$$g_{t+1} = \begin{cases} \pi_m(s_t) & \text{if } t \bmod k = 0 \\ s_t + g_t - s_{t+1} & \text{otherwise} \end{cases} \quad (50)$$

E.4 Reproducibility of the HIRO algorithm

Our implementation of HIRO, in particular the use of egocentric goals and off-policy corrections as highlighted in the original paper, are adapted largely from the original open-sourced implementation of the algorithm, as available in <https://github.com/tensorflow/models/tree/master/research/efficient-hrl>. Both our implementation and the original results from the paper exhibit similar improvement when utilizing the off-policy correction feature, as seen in Figure 6, thereby suggesting that the algorithm was successfully reproduced. We note, moreover, that our implementation vastly outperforms the original HIRO implementation on the Ant Gather environment. Possible reasons this may be occurring could include software versioning, choice of hyperparameters, or specific differences in the implementation outside of the underlying algorithmic modification. More analysis would need to be performed to pinpoint the cause of these discrepancies.

E.5 Hierarchical Actor-Critic with egocentric goals

To ensure that the hindsight updates proposed within the HAC algorithm are compared against other algorithms on a level playing field, we modify the non-primary features of this algorithm to result in otherwise similar training performance. For example, while the original HAC implementation utilizes DDPG as the underlying optimization procedure, we use TD3. Moreover, while HAC relies on binary intrinsic rewards that significantly sparsify the feedback provided to the worker policy, we on the other hand use distance from the goal.

We also extend the Hierarchical Actor-Critic (HAC) algorithm presented by [6] to support the use of relative position, or egocentric, goal assignments as detailed in Appendix E.3. This is done by introducing the goal-transition function $h(\cdot)$ to the hindsight goal computations when utilizing hindsight goal and action transitions. More concretely, while the original HAC implementation defines the hindsight goal \tilde{g}_t at time t as $\tilde{g}_t = \tilde{g}_{t+1} = \dots = \tilde{g}_{t+k} = s_{t+k}$, the hindsight goal under the relative position goal assignment formulation is $\tilde{g}_{t+i} = s_{t+k} - s_{t+i}$, $i = 0, \dots, k$. This function results in the final goal \tilde{g}_{t+k} before a new one is issued by the manager to equal zero, thereby denoting the worker’s success in achieving its allocated goal. These same goals are used when computing the intrinsic (worker) rewards in hindsight.

F Additional results

F.1 Compositionality with existing algorithms

We find that the use of cooperative manager gradients can improve the training performance of existing techniques. Figure 7 demonstrates this for the Ant Gather. As we can see, the use of CHER-style manager updates assists in improving the performance of the HAC algorithm; however, this

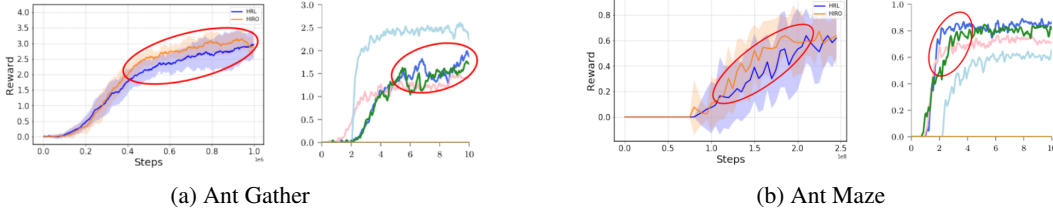


Figure 6: Training performance of the original implementation of the HIRO algorithm with ours. The original performance of HIRO, denoted by the right figure within each subfigure, is adapted from the original article, see [3]. While the final results do not match exactly, the relative evolution of the curves exhibit similar improvements, as seen within the regions highlighted by the red ovals.

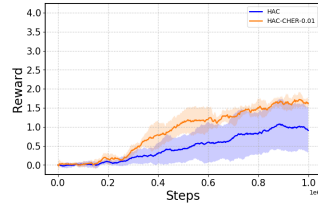


Figure 7: Performance of HAC when coupled with CHER on the Ant Gather environment.

algorithm is still unable to match the performance of solely using CHER. Further analysis is required to identify which combination of methods would yield optimal results for different environments.

F.2 Visual Ant Maze

Shown by figure 8, CHER performs comparably to HIRO when trained on an image-based variant of our Ant Maze environment. In this particular environment, the XY position of the agent is removed from its observation. Instead, a top down egocentric image is provided to the agent, colored such that the agent can recover the hidden XY positions as a nonlinear function of image pixels. Perhaps more interesting, while CHER achieves competitive performance with HIRO, CHER trains moderately faster than HIRO, which is shown in Figure 9. This is likely due to not requiring goal off policy relabelling at every step of gradient descent for the manager policy.

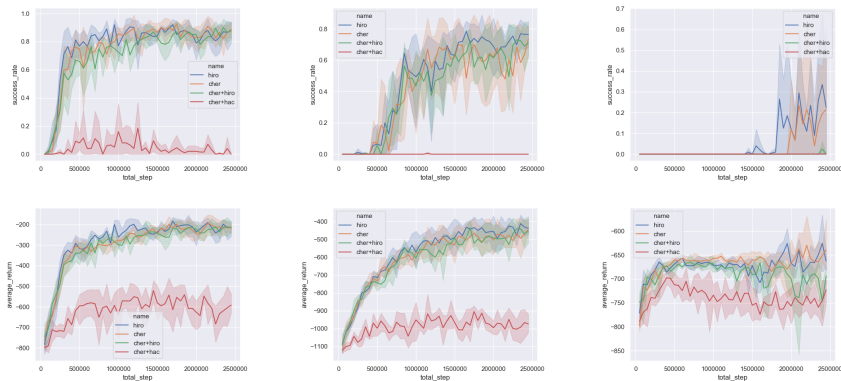


Figure 8: This figure shows the success rates, measured when the agent's center of mass enters within ϵ units to the goal position, and an average return, calculated as the sum of negative distances from the agent's center of mass to the goal position. Total steps indicates the number of samples taken from the environment.

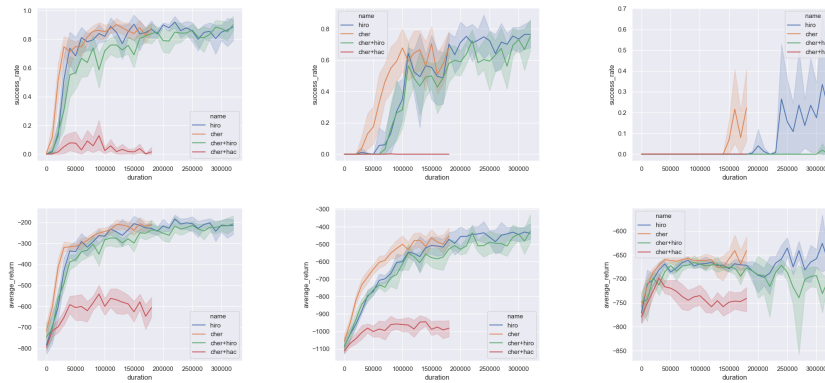


Figure 9: This figure shows the success rates, measured when the agent's center of mass enters within ? units to the goal position, and an average return, calculated as the sum of negative distances from the agent's center of mass to the goal position. Unlike figure 8, the x-axis in these plots is the duration of the experiment, measured by the wall clock time in seconds from start to 2.5 million environment steps.